

# Modelling Hole Transport in Slithering-Snake Simulated Blends of Conjugated Polymers

Jenny Nelson, Jarvist Frost

September 8, 2005

# Abstract

Blends of conjugated polymers were simulated by using a slithering-snake Monte-Carlo algorithm. Two distinct three-dimensional structures arose, depending whether the polymers were homophilic or heterophilic. Time of flight simulations were carried out with no energetic disorder, in order to try and isolate the effect of morphology.

Homophilic polymers formed clumps, and it was demonstrated that a quasi-equilibrium existed between local clumping and full phase separation, which we believe is most indicative of experimental samples. The size of clumps in this quasi-equilibrium was found to be highly temperature dependent. Time of flight simulations produced dispersive transients with positive mobility dependency on field.

Heterophilic polymers demonstrated a stable ‘lacework’ pattern for densities of above 16%. These structures offered enormous interfacial area between the two polymers, and very low diffusion distances for an exciton to travel before reaching a boundary. Time of Flight simulations indicated non-dispersive (charge-sheet like) behaviour at low bias, which then became more dispersive as the bias increased. This was understood in terms of the high bias causing ‘fish trap’ structures to appear where the carriers were trapped in ‘downstream’ but non connecting regions.

## 1 Introduction

## 2 Morphology Generation

Morphologies were generated by use of a Slithering-Snake monte carlo method. A population of conjugated polymer chains (snakes) were drawn from a Gaussian distribution of chain length with associated parameters  $\bar{l}$  &  $\sigma_l$ , and then laid down randomly in the 3D lattice.

These polymer chains were constricted to move linearly, with one of the heads extending itself by one unit in any of the three cartesian directions. They were considered to be in a ‘sea’ of other material, which was displaced around the snake without energy cost.

For each ‘slither’ of the monte-carlo simulation, a particular snake, head and direction were chosen at random. A calculation was made of the energy change associated with such a move, which came about as a result of the interaction energies between lattice units of ‘snake’ [conjugated polymer oligomers] versus the ‘sea’ of other plastic or the snake material itself.

Due to the constrictions placed on the snake movement, and once consideration was made for the energy associated with a configuration where a certain

snake touched itself, this calculation could be simplified to a energy summation over the lattice site that the ‘head’ was about to move into, and the site that the ‘tail’ was about to depart from. This calculation is independent of chain length.

When this energy,  $dE$ , was negative then the exothermic movement progressed automatically. For  $dE > 0$ , the endothermic movement progressed if there was sufficient Boltzman energy to drive it.

## 3 Morphology Results

Two fundamentally different morphologies were generated by setting the Snake-Snake interaction energy either positive or negative, generating homophilic and heterophilic polymer chains respectively. Due to the THATOTHERDUDESNAME principle, a homophobic blend is equivalent to a heterophilic one - where the polymers would energetically prefer to be in touch with each other. A homophilic blend would be expected to phase phase separate, whereas a heterophilic blend would prefer to be in a stable blend.

The percolation threshold of the two different blends was examined [Fig. 3], and was found to be different for the two morphologies. Homophilic blends went through a percolation boundary at between 20 – 30%, whereas heterophilic blends began

percolating at between 16 – 25%.

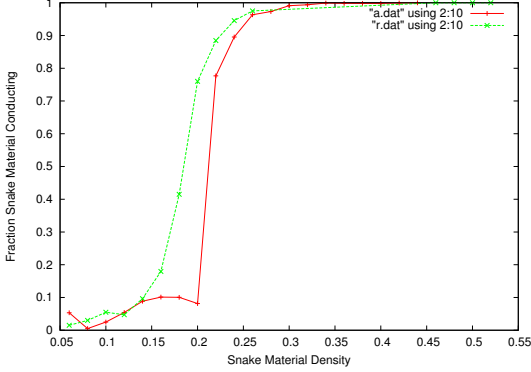


Figure 1: Figure displaying the fraction of segments connected to the base electrode by a percolating cluster, versus the density of the mix, for both homophilic & heterophilic snakes.

### 3.1 Homophilic Blends (Clumping)

When the snake-snake affinity was greater than the snake-sea material, clumping into separate islands of material was observed. Initial clumping is very fast, producing small islands ( $\approx 10$  tangled snakes) that display a collective mobility which produces in the medium term large islands ( $\approx 100$  tangled snakes) [Fig. 2(a)]. These large islands are fairly immobile, and further aggregation is achieved by a periodic ejection of small numbers of snakes ( $\approx 1 - 4$  snakes) which are then free to wander around the lattice, until becoming associated with another island. This, extremely slow, aggregation eventually produces a full phase separation of the material, wherein the small islands eventually ‘evaporate’, forming one large tangle of snakes.

We believe that experimental samples exist somewhere in the middle-part of the above process, where a quasi-equilibrium exists. Complete aggregation and phase separation takes several more decades of time than achieving the local-clumping.

At lower temperatures, this clumping occurs on a more local scale producing smaller sized clumps distributed across the lattice. As the temperature increases, the clumps become larger. Once  $k_b T \gg E_{int}$ ,

the clump size decreases and the morphology tends towards a random distribution of snakes.

We found that  $k_b T \approx E_{int}$  gave rise to the most clumped material, and approached quasi-equilibrium fastest. Therefore a figure of  $k_b T = E_{int}$  was used to generate the majority of simulated samples, in order to show maximum diversity between the two morphologies.

### 3.2 Heterophilic Blends (Lacework Pattern)

When the affinity between snake-sea was made greater than that for snake-snake, it had been anticipated that the snakes would avoid each other and produce a poorly percolating structure. This was indeed demonstrated to be true for low densities ( $< 15\%$  in 3D), where the ‘snakes’ kept themselves separated from one another. However, as the density was increased, some interesting behaviour emerged. Initially, the increase in density meant that a random assembly of rods would interact - and so the polymer chains adopted a loose-spiral formation.

As the density increased further, the chains were forced into a touching lacework configuration [Fig. 2(b)]. This structure provides enormous interfacial area between the two polymers in the blend, which we note may have implications for the exciton lifetime before disassociation into Hole-Electron pair & rates of recombination.

Again, excessive temperatures produced a random distribution, and at low temperatures the blends took a long time to settle into a lacework structure. A figure of  $E_{int} = |k_b T|$  was found to produce the minimally clumped blend in the shortest time.

## 4 CTRW Time of Flight

A Continue Time Random Walk (CTRW) was used to simulate a Time of Flight experiment using synthesised blends of the two polymers generated above. A collection of charge carriers (typically 200) were generated randomly in the first 10% of the vertical extent of the sample (typical dimensions  $1000 \times 50 \times 50$ ). The hoppers were constricted to move only within

one type of polymer in the blend. Charge movement was by short range hopping of the charge carriers to unoccupied lattice sites.

In a CTRW, a list is kept of such ‘hoppers’ with their respective time until they tunnel, and destination. The simulation time is advanced to that of the first hopper to move, which is then moved to its intended lattice location. Any movement with or against the field is considered a contribution to the current, which was collated into geometric time bins. The hopper then has the next ‘hop’ chosen, and is reinserted into the queue.

When hoppers reached the far end of the lattice, they were considered to have been picked up by the electrode, and were removed from the simulation.

For each lattice site, the rate of hopping between near neighbours were calculated by using THATDUDESNAME formalism, considering a uniform electric field across the lattice. These rates, along with a summation of the total hopping rates, were computed for all lattice sites and cached for later lookup. Energetic site disorder was not considered, in order to isolate the effects of morphology, and a figure of  $0.5\text{eV}$  was used for the  $\lambda$  site deformation energy.

$$\gamma = \gamma_0 e^{-\frac{(\delta E)^2}{4\lambda k_b T} - \frac{r}{r_0}}$$

Where the simulation was run at a temperature  $T = 300\text{K}$ , and with a tunneling parameter of  $r_0 = 0.15$  lattice sites.

Each hopper was given a certain wait time by:

$$\delta t = -\ln\left(\frac{X}{\gamma_{total}}\right)$$

Where  $X$  is a random number between  $0 \rightarrow 1$ , and  $\gamma_{total}$  is the summation of rates for that lattice site.

The destination for the hopper was chosen by selecting randomly from the collection of possible jumps, weighted by the relative magnitude of the rate. If the destination site was found to be occupied by a hopper, another destination was randomly chosen. If the hopper was found to be trapped by surrounding hoppers, a ‘phantom’ hop was inserted into the queue, whereby the hopper ‘moved’ to its on location at a future time, allowing hoppers to ‘sleep’ until a time by which the surrounding hoppers would have moved away.

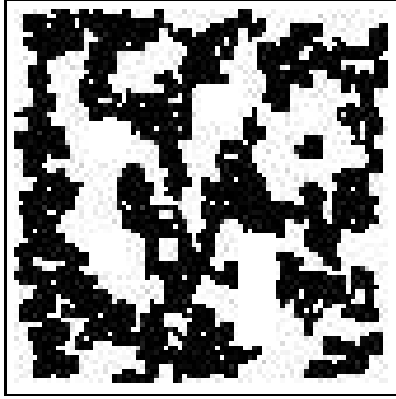
## 5 Time of Flight Results

Testing was done with a pure 100% sample, which displayed the expected charge-sheet like behaviour and positive field-dependence of mobility. Simulations were then made with the prepared  $1000 \times 50 \times 50$  blends of homophilic & heterophilic polymer chains at a variety of densities. The electric field bias was varied from 0.01 to 0.1 eV/site, which along with the 1000 unit thick lattice, was intended to simulate a  $1000\text{nm}$  thick blend of conjugated polymer with biases of 10 to 100V.

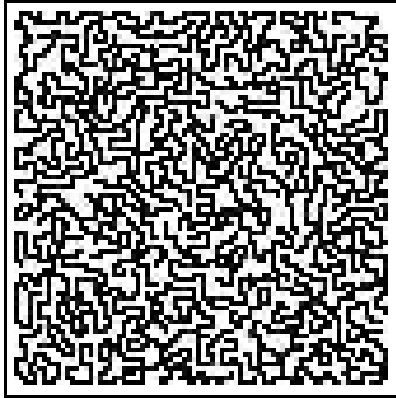
The Heterophilic morphology was found to produce non-dispersive ‘charge-sheet’ ToF transients, which became more dispersive as the bias was increased. This was understood by the existence of ‘fish-trap’ structures within the morphology. High density morphologies were found to be increasingly resistive to this deformation into dispersive transport. Densities above 17% were found to produce conducting films.

Homophilic morphologies only produced viable ToFs for densities of above 22%. Low ( $< 35\%$ ) density morphologies gave rise to entire dispersive transport at the range of biases sampled, but higher densities exhibited similar though less pronounced field-responsive dispersive transport.

## 6 Conclusions

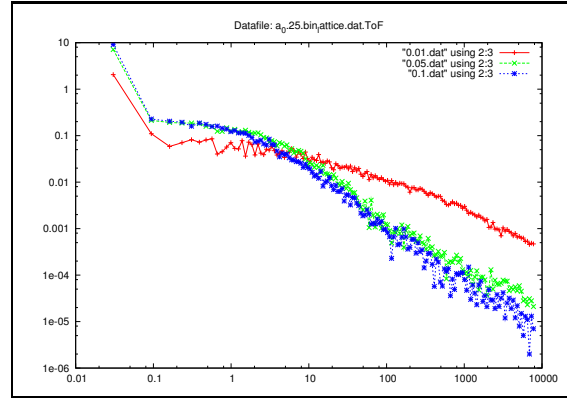


(a) Homophilic (Clumping)

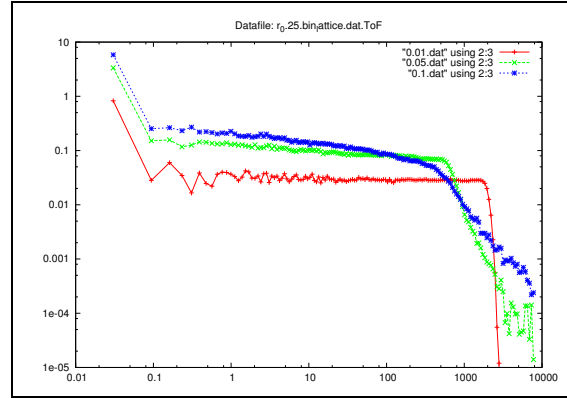


(b) Heterophilic (Lacework Pattern)

Figure 2: 2D morphologies generated on a  $80 \times 80$  lattice using 25 unit snakes, at a 50% by volume density. Simulations were run to quasi-equilibrium. Identical simulation parameters were used for both, except for the sign of the snake-snake affinity.



(a) Homophilic (Clumping)



(b) Heterophilic (Lacework Pattern)

Figure 3: Simulated Time of Flights generated from 25% density homophilic & heterophilic polymer blends. Current versus Time is presented on a logscale, with the data collated into 150 geometric timebins. Three biases are displayed, 0.01, 0.05 & 0.1  $eV/site$ .